Vol. 730: 43–58, 2024
https://doi.org/10.3354/meps14525

MARINE ECOLOGY PROGRESS SERIES
Mar Ecol Prog Ser

Published March 7

Mitochondrial and morphological adaptions of *Lindaspio polybranchiata* (Annelida: Spionidae) in the South China Sea

Yujie Yan[1,2], Minxiao Wang[1], Xuwen Wu[3], Haining Wang[1,2], Zhaoshan Zhong[1], Chaolun Li[1,2,4,*]

[1]CAS Key Laboratory of Marine Ecology and Environmental Sciences, and Center of Deep Sea Research, Institute of Oceanology, Chinese Academy of Sciences, Qingdao 266071, PR China

[2]University of Chinese Academy of Sciences, Beijing 100049, PR China

[3]Laboratory of Marine Organism Taxonomy and Phylogeny, Qingdao Key Laboratory of Marine Biodiversity and Conservation, Institute of Oceanology, Chinese Academy of Sciences, Qingdao 266071, PR China

[4]South China Sea Institute of Oceanology, Chinese Academy of Sciences, Guangzhou 510301, PR China

ABSTRACT: A dense population of *Lindaspio polybranchiata* (Annelida: Spionidae) was discovered in a novel cold seep with drastic methane seepage located on the northern passive continental margin of the South China Sea. *L. polybranchiata* may function as a pioneer species by rapidly colonizing this nascent methane seep. We studied its classification status and evolutionary selection adaptation based on the mitochondrial genome. Phylogenetic analysis revealed that the deep-sea genus *Lindaspio* clustered with the neritic *Rhynchospio* aff. *asiatica*, and the ancestor of the deep-sea *Lindaspio* might originate from shallow-water spionids. Twelve potentially adaptive mutations were identified in *cox1*, *cox3*, *cytb*, and *nad5*. The morphological characteristics of *L. polybranchiata* and *R.* aff. *asiatica* collected in the intertidal zones were systematically compared to explore the possible phenotypic adaptations of *L. polybranchiata* to extreme deep-sea environments. *L. polybranchiata* lost its eyespots due to long-term colonization of the dark habitat in the deep sea but developed an enlarged caruncle for facilitating chemical perception in the darkness. The specific ventral branchiae and extended respiratory surfaces may aid the survival of *L. polybranchiata* in the hypoxic environment of the cold seep. This study provides novel insights into the molecular and morphological adaptations of a species endemic in chemosynthetic ecosystems.

KEY WORDS: Deep-sea polychaetes · Mitogenome · Phylogenetic study · Positive selection · Morphological adaptation

1. INTRODUCTION

Polychaetes are common organisms in the deep sea, where they are highly abundant and play important ecological roles in deep-sea chemosynthetic ecosystems (Desbruyeres & Toulmond 1998, Blake 2000, Sellanes et al. 2004, Reuscher et al. 2012). Some vestimentiferan polychaetes are regarded as ecosystem engineers of newly opened vents, as they promote habitat complexity and stimulate colonization by other species (Shank et al. 1998, Hunt et al. 2004, Hilário 2005, Cordes et al. 2009). A series of studies has investigated the morphological characteristics (Reuscher et al. 2012, Han et al. 2021, Alalykina 2022) and species diversity (Guggolz et al. 2019, 2020) of deep-sea polychaetes. However, limited information is available about the origin, phylogenetic status, and evolutionary adaptations of these ecologically important groups to date (Fontanillas et al. 2017, Sun et al. 2021).

*Corresponding author: lcl@qdio.ac.cn

Deep-sea chemosynthetic ecosystems are usually characterized by low oxygen availability due to high leakage of methane-rich fluids (Boetius & Wenzhöfer 2013). Mitochondria are important organelles for aerobic respiration, and the mitochondrial respiratory chain complex produces up to 95% of the energy in eukaryotic cells. Therefore, extreme deep-sea environments are likely to affect the mitochondrial genome and its encoded metabolic processes. It is likely that mitogenomes are subject to evolutionary selection to meet metabolic demands in extremely harsh environments (Nakajima et al. 2016). The first example of genetic rearrangement was observed in the transfer RNA (tRNA) genes of a deep-sea fish, *Gonostoma gracile* (Miya & Nishida 1999). The mitochondrial gene orders of deep-sea bathymodioline mussels are significantly different from those of shallow-water mussels, and 16 residues of *atp6*, *nad4*, *nad2*, *cytb*, *nad5*, and *cox2* have undergone positive selection, indicating possible adaptation to the deep-sea environment (Zhang et al. 2021).

In addition to mitochondrial evolution, deep-sea organisms also exhibit morphological, physiological, and metabolic adaption to extreme environments. The presence of sulfides, toxic hydrocarbons, and heavy metals can disrupt essential biological processes. The giant tubeworm genus *Riftia* possesses metallothionein-like proteins and hosts symbiotic bacteria that are involved in the detoxification of high levels of sulfide and heavy metals in the worms' tubes (Hourdez & Jollivet 2020, Lo Giudice & Rizzo 2022). Regarding hypoxia and the universal deep-sea stress, polychaetes have an enlarged respiratory organ to increase oxygen extraction capacity (Storch & Alberti 1978, Hourdez et al. 2001), modified respiratory pigments to improve oxygen transport efficiency (Hourdez et al. 2002, Hourdez & Lallier 2007), and enhanced respiratory enzyme activity to improve oxygen utilization (Quiroga et al. 2007, Rinke & Lee 2009). Several sense appendages of polychaetes also undergo adaptive evolution under selection pressure due to the persistent darkness. Most polychaetes collected near the deep-sea hydrothermal vents in the Eastern Pacific all possessed well-developed peristomial rings and enormous palps that served as sensory replacements for sightless animals in the deep sea (Blake 1985).

The family Spionidae is one of the largest and most common polychaete families in marine benthic invertebrate communities, and comprises approximately 590 species belonging to 38 genera (Radashevsky 2012). Spionids are regarded as opportunistic species with a low reproductive age, high fecundity, and short life span (David & Williams 2012, Bennett & Rakocinski 2020). The strong dispersal ability of the larvae and the r-selected life-history pattern have allowed spionids to rapidly invade new habitats and emerge as dominant species in several benthic communities (Conlan & Kvitek 2005, Birch et al. 2018). For instance, a previous study reported the successful invasion by *Marenzelleria* spp. in the species-poor ecosystem of the Baltic Sea and their subsequent spread throughout the entire Baltic Sea (Kauppi et al. 2015). An increasing number of highly abundant spionid taxa have been recently discovered in deep-sea chemosynthetic ecosystems (Hourdez et al. 2006, Graff et al. 2008, Blake & Ramey-Balci 2020). The genus *Lindaspio* is an especially interesting taxon of the family Spionidae, and all *Lindaspio* species have been reported to dwell in chemosynthetic environments, including hydrothermal vents, hydrocarbon seeps, and whale falls (Blake & Maciolek 1992, Bellan et al. 2003, Sumida et al. 2016, Sui et al. 2023). However, studies on spionids dwelling in deep-sea chemosynthetic ecosystems are limited to species diversity and distribution (Blake & Maciolek 1992, Sigvaldadóttir & Desbruyeres 2003, Bogantes 2020, Guggolz et al. 2020), and little is known about the evolutionary history and environmental adaptability of this group.

A novel methane vent area named Lingshui was discovered in May 2021 on the northern passive continental margin of the South China Sea (SCS). The concentration of methane in the surface sediments of the biological zones ranged from 0.79 to 5.09 mmol l^{-1} (L. Cao unpubl. data), and massive methane bubbles could be seen gushing from the seafloor at this site. The *in situ* dissolved oxygen of the water–sediment interface was approximately 2.96 mg l^{-1} (L. Cao unpubl. data). Around the active vent, we discovered dense aggregations of *L. polybranchiata* (Sui et al. 2023). As almost no other animals have been found in this area besides this species, we speculated that *L. polybranchiata* may be a pioneer species of this nascent methane vent. In this study, we investigated mtDNA variation patterns, tried to reconstruct the evolutionary pathways of the deep-sea *Lindaspio*, and investigated how *Lindaspio* adapted to the deep-sea environment from the perspective of the mitogenome. *Lindaspio* was recovered as a sister taxon to *Rhynchospio* by combined analyses of whole-genome sequencing (WGS) data and transcriptome data of 29 species covering 17 spionid genera (Bogantes 2020). Thus, we compared *L. polybranchiata* with an intertidal spionid, *Rhynchospio* aff. *asiatica*, to explore how deep-sea polychaetes survive in extreme environments, especially in dark and oxygen-limited environments. The

results may provide primary insights into the mitochondrial and morphological adaptations of the family Spionidae to extreme deep-sea environments.

2. MATERIALS AND METHODS

2.1. Sample collection and preservation

Lindaspio polybranchiata was sampled in May 2021 by the ROV 'Faxian' from the sediment around the seepage (1800 m) in the SCS (Fig. 1A). Specimens were collected by TV-guided grab sampler and push-core sampler to estimate the population density at the sampling sites depicted in Fig. 1B. The animals were rinsed several times with Milli-Q water to remove the attached sediments. Some specimens were then snap-frozen in liquid nitrogen and preserved in a −80°C freezer for subsequent molecular analyses, and others were fixed in 2.5% glutaraldehyde for morphological observations.

Rhynchospio aff. *asiatica* was collected from intertidal sediments at Qingdao Bay (36.060° N, 120.320° E) in November 2021 (Fig. 1A). After rinsing off the sediments with seawater, the samples were transferred to plastic bottles containing seawater. Specimens of *R.* aff. *asiatica* were selected under a stereoscopic microscope (SteREO Discovery V20, Zeiss) and preserved with the same methods as *L. polybranchiata.*

2.2. DNA extraction, sequencing, assembly, and annotation

The total genomic DNA of *L. polybranchiata* (n = 8) and *R.* aff. *asiatica* (n = 1) was extracted using the E.Z.N.A.® Mollusc DNA kit (OMEGA Bio-Tek) and sequenced on an Illumina Hiseq 2500 system (2×150 bp pair-end reads). The mitogenomes were de novo assembled by the MitoZ toolkit (Meng et al. 2019) with default parameters. Gene annotation was performed using the MITOS2 web server (Bernt et al. 2013) and the manual refinement method based on the Open Reading Frame Finder prediction combined with the results of the Basic Local Alignment Search Tool against the NCBI nr database. Finally, the mitochondrial genome map was obtained in the CGview server (https://proksee.ca/). In addition to the mitogenomes obtained, the WGS data of *Lindaspio* sp. collected at 1130 m at New England Seep 2 (NES) (SRR13436066) were retrieved and analyzed following the aforementioned pipeline. All sequences have

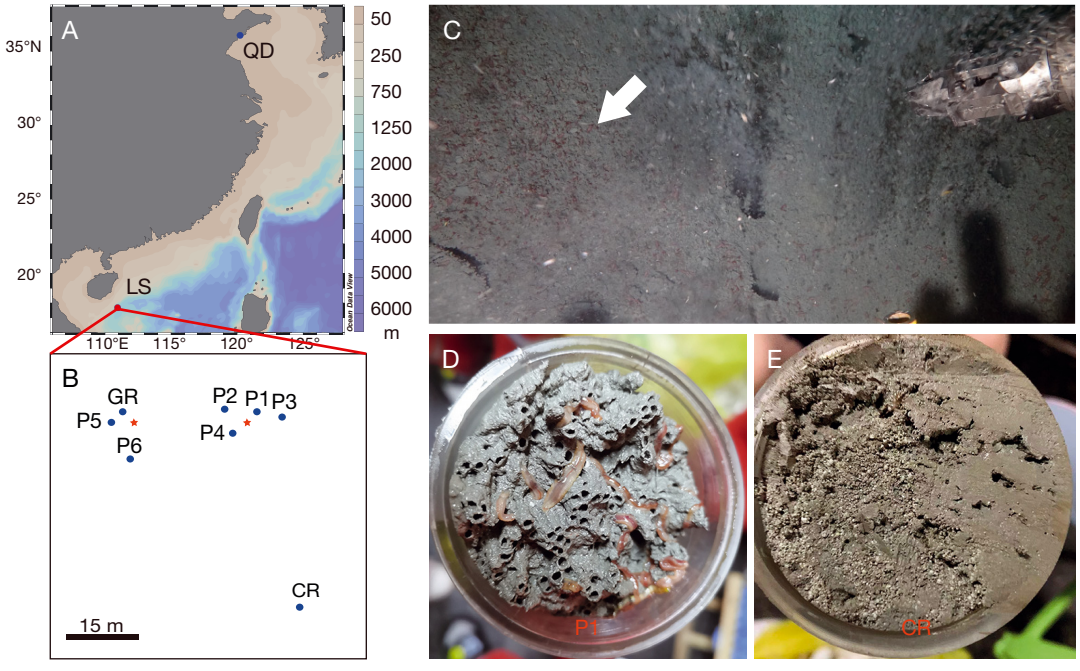

Fig. 1. Characteristics of the sampling stations. (A) Locations of the sampling stations. QD (Qingdao Bay): sampling station for *Rhynchospio* aff. *asiatica*; LS (Lingshui): sampling station for *Lindaspio polybranchiata.* (B) Sampling sites in Lingshui, where a TV-grab (site GR) and a push-core sampler (sites P1−P6, CR) were used. The methane vents are indicated by red stars. (C) *In situ* photograph showing an aggregation of *L. polybranchiata* (white arrow) with massive overflowing methane bubbles. (D) Surface sediment at site P1, indicating the habitat of *L. polybranchiata.* (E) Surface sediment at site CR, with *L. polybranchiata* absent

been deposited in GenBank under accession numbers OK032597 (*L. polybranchiata*), BK062759 (*Lindaspio* sp. [NES]), and OP288981 (*R.* aff. *asiatica*).

2.3. Phylogenetic analysis

To determine the phylogenetic position of *L. polybranchiata* with respect to other polychaetes, the complete mitochondrial genomes of 29 polychaetes including 5 orders and *Magelona mirabilis* and *Owenia fusiformis* (serving as the outgroup) (Chen et al. 2020) were used to conduct a phylogenetic analysis (Table S1 in Supplement 1 at www.int-res.com/articles/suppl/m730p043_supp1.xlsx). The maximum likelihood (ML) tree with the GTR model was constructed using RaxML (Stamatakis 2014). Node confidence was assessed using 1000 bootstraps. Codon usage analysis, base constitutions, and the genetic divergence (Kimura 2-parameter [K2P] distance) between 2 species were analyzed in MEGA11 (Tamura et al. 2021).

2.4. Estimation of divergence time

The ML tree and the GTR nucleotide substitution matrix were used to construct the divergence tree using MCMCTree (Yang & Rannala 2006) to estimate the divergence time between the deep-sea *Lindaspio* and other shallow-water spionids. Three nodes were calibrated with the following fossil times: Magelonidae–Oweniidae appeared around 514 million yr ago (Ma) (Chen et al. 2020); Errantia and Sedentaria diverged between 120 and 493 Ma (Peterson 2005); and *Sclerolinum* appeared around 8.19 Ma (www.timetree.org/). For Markov chain Monte Carlo (MCMC) analysis, 2 runs were performed with nburn-in = 200 000, nsamfreq = 10, and nsample = 500 000. The convergence of sampled parameters and possible autocorrelation (effective sampling size for all parameters >200) were calculated using Tracer 1.6 (http://tree.bio.ed.ac.uk/software/tracer/). The branch lengths were highly consistent between the 2 runs, and the total percentage of bias in the branch lengths was <0.1%.

2.5. Population genetic analysis

The mitogenomes of 8 individuals were used for population genetic analysis. These specimens were sampled from sampling sites GR, P3, and P5 (Fig. 1B) that covered the distribution zones of *L. polybranchiata.* To gain insights into the population genetic variability and structure of *L. polybranchiata*, several descriptive indices, including nucleotide diversity (Pi), haplotype diversity (Hd), and polymorphic sites, were calculated for the 13 concatenated protein-coding genes (PCGs; 11 105 bp) of the 8 individuals using DnaSP v6 (Rozas et al. 2017). Furthermore, Tajima's D, Fu and Li's D^*, and Fu's F_S test statistics were determined using DnaSP to test the hypothesis of random deviation from neutral evolution and potential population expansion. A pairwise mismatch distribution analysis was performed in Arlequin v3.1 (Excoffier et al. 2006) to determine the population dynamics and infer the demographic history of *L. polybranchiata*.

2.6. Positive selection analysis

A phylogenetic tree with only 6 spionids and 2 terebellids was subsequently constructed for analyzing positive selection. The genes and sites under positive selection were identified using the CodeML program in the pamlX package (Yang 2007). The clades consisting of *Lindaspio* species were marked as the foreground branch with other spionids serving as the background. The branch model was implemented to identify whether the foreground branch evolved significantly faster than the background branch. Branch-site model analyses were performed to determine the sites under positive selection in the mitochondrial genes of the *Lindaspio* lineage. Chi-squared tests were performed, and $p < 0.05$ indicated rejection of the null hypothesis of neutrality.

To explore the effect of these putative sites, PredictProtein was used to identify the structures and functions of the positively selected genes (Yachdav et al. 2014). TMHMM 2.0 (https://services.healthtech.dtu.dk/service.php?TMHMM-2.0) was also used to determine whether these sites were situated in the transmembrane region. The 3D structure of these positively selected PCGs was constructed by SWISS-MODEL (https://swissmodel.expasy.org), and the positively selected residues were mapped to the corresponding genes (see Fig. S4).

2.7. Morphological observations

The specimens of *L. polybranchiata* and *R.* aff. *asiatica* were mounted and observed under a stereoscope (SteREO Discovery V20, Zeiss) to record the key morphological features and obtain some quantitative data, including body width (width of the fifth body

segment) and body length (number of body segments) (Table S2). About 20% of the right parapodia of the polychaetes were randomly dissected along the body axis to calculate the total area of the gills (see Fig. 5A,B). The projection area of the gill plane was measured based on the picture scale, and its mean value was calculated. As the bodies of spionids are symmetrical, and their gills are approximately cylindrical, the total surface area of gills was calculated using the following formula: total gill area = average projection area of gill plane × the number of gills × 3.14 (Hourdez et al. 2001).

The morphological details were obtained by scanning electron microscopy. The fixed samples were washed 3 times with 1× phosphate-buffered saline (PBS, Thermo Fisher) and subsequently dehydrated in different concentrations of ethanol (30, 50, 70, 80, 90, and 100%), for 15 min at each concentration. The samples were placed in isoamyl acetate and dried with a CO_2 critical point dryer (EM CPD 300, Leica) and sputter-coated with gold (Sputter/Carbon Thread, EM ACE200, Leica). The prepared samples were finally observed under a scanning electron microscope (S-3400N, Hitachi).

3. RESULTS

3.1. Characteristics of the benthic community around the active vent in Lingshui

Lindaspio polybranchiata was found at a newly discovered active methane seep in the SCS. In the survey area, we observed many bubbles gushing from the seafloor by ROV, and there were no visible epifauna on the surface of sediments around the seepage (Fig. 1C). A detailed investigation was launched in this area. TV-grab sampling revealed that the macrofauna were dominated by polychaetes. Among several polychaetes, a large worm, *L. polybranchiata*, numerically dominated the sample with an abundance of 8010 ind. m^{-2}. The other polychaetes could not be identified, as they were small and became fragmented after flushing, and their abundance was more than an order magnitude less than that of *L. polybranchiata*. The distribution was also determined in detail by random push-core sampling at several sites around the seepage (Fig. 1B). Only *L. polybranchiata* was found in the push-core samplers around the seepage, and their abundance was estimated to be 3977–34 465 ind. m^{-2} (Table 1). *L. polybranchiata* burrowed in the sediments, secreted mucus for gathering the sediment particles, and formed loose tubes (Fig. 1D), and their depth distribution in the sediments could reach more than 30 cm. However, no *L. polybranchiata* were found in locations more than 50 m away from the area of the vent (Fig. 1E).

3.2. Mitochondrial adaptations of *Lindaspio polybranchiata*

3.2.1. Features of the mitochondrial genome

The mitochondrial genomes of *L. polybranchiata* and *Rhynchospio* aff. *asiatica* were sequenced and assembled. The length of mitogenomes of *L. polybranchiata* ranged from 15 248 to 15 416 bp. The 15 248 bp long sequence was used for downstream analyses. The mitogenome contains 13 PCGs, 21 tRNAs (tRNA Gln absent), 2 ribosomal RNAs (rRNAs), and 1 control region (CR) (Table S3). The characteristics of the mitogenome of *L. polybranchiata* are presented in Fig. 2. The overall base composition was 28.4% A, 23.6% C, 13.0% G, and 34.9% T, revealing a high A+T content (63.3%). The AT-skew and GC-skew were both negative, being −0.10 and −0.29 respectively.

The total length of 13 PCGs was 11 105 bp, with A+T content of 61.8%. The gene order of 13 PCGs is *cox3-nad6-cytb-atp6-nad5-nad4l-nad4-nad1-nad3-nad2-cox1-cox2-atp8*. The genes *cox3* and *atp6* use ATA as the start codon, and all other PCGs use ATG as the start codon. Most of the PCGs terminate with the stop codon TAA, whereas *cytb* terminates with TAG, and *nad4*, *nad1*, and *cox1* terminate with an incomplete stop codon T-. The 3 most common codon usages were Ile (codons per thousand codons [CDspT]: 125.53), Leu2 (CDspT: 117.44), and Phe (CDspT: 91.42) (Fig. S1 in Supplement 2 at www.int-res.com/articles/suppl/m730p043_supp2.pdf). Relative synonymous codon usage analysis revealed that the third codon position tends to be A and T

Table 1. Abundance of *Lindaspio polybranchiata* at the sampling sites at Lingshui (see Fig. 1)

	Sampling site							
	PC1	PC2	PC3	PC4	PC5	PC6	GR	CR
Abundance (ind. m^{-2})	7291	20547	17895	25186	3977	34465	8010	0

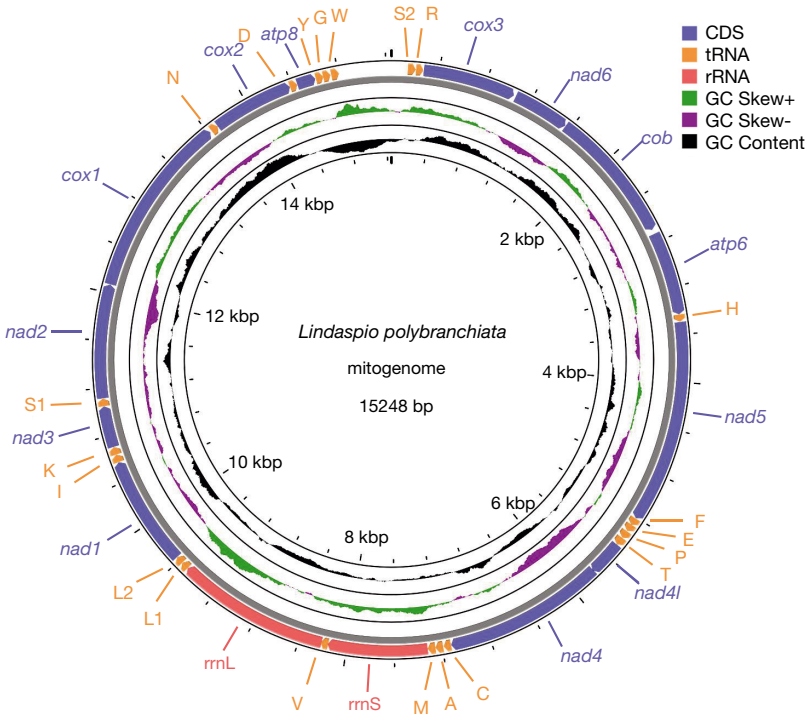

Fig. 2. Mitochondrial gene map of *Lindaspio polybranchiata*. The direction of the arrows indicates the direction of gene transcription. The protein-coding genes and rRNAs are shown with standard abbreviations, and the tRNA genes are denoted by a single letter according to International Union of Pure and Applied Chemistry–International Union of Biochemistry abbreviations (i.e. L1: CUN; L2: UUR; S1: AGN; S2: UCN) (https://iupac.qmul.ac.uk/AminoAcid/A2021.html)

(Fig. S1). The pairwise divergence among the mitogenomes of Spionidae was calculated based on the 13 concatenated PCGs. The results showed that *L. polybranchiata* had the lowest nucleotide divergence of 0.26% (K2P distance) with *Lindaspio* sp. (NES). The pairwise divergence between *L. polybranchiata* and *Polydora hoplura* was the highest, with a K2P distance of 69.85% (Table S4).

3.2.2. Phylogenetic analysis

We constructed phylogenetic trees using amino acid sequences of 12 concatenated PCGs and nucleotide sequences of 12 PCGs and 2 rRNAs to provide evolutionary relationships. The topologies of the 2 phylogenetic trees were consistent, and the phylogenetic tree constructed with nucleotide sequences (Fig. 3) has higher support at each node compared to that with amino acid sequences (Fig. S2). Phylogenetic analysis confirmed the monophyly of Errantia and Sedentaria. The ML tree also strongly supported the monophyly of Spionidae, Siboglinidae, and Terebelliformia in Sedentaria. In the phylogenetic tree with nucleotide sequences, the Spionidae were closely related to Siboglinidae with good support (bootstrap value: 100). The phylogenetic analysis revealed that *L. polybranchiata* from Lingshui was recovered as a sister to *Lindaspio* sp. from New England seep 2, with good support (bootstrap value: 100). Together, these 2 species of *Lindaspio* formed a well-supported clade that was a sister to the clade formed by *Marenzelleria neglecta* and *R.* aff. *asiatica* (bootstrap value: 100) (Fig. 3).

Estimation of divergence time showed that Spionidae diverged at approximately 364.37 Ma (95% confidence interval: 258.25–490.45 Ma) from Siboglinidae (Fig. 3). Within Spionidae, the deep-sea genus *Lindaspio* diverged from other shallow-water spionids at around 208.09 Ma (95% confidence interval: 116.33–297.89 Ma). *L. polybranchiata* at the Lingshui cold seep and *Lindaspio* sp. at New England seep 2 diverged at 2.03 Ma (95% confidence interval: 0.36–4.32 Ma).

The mitochondrial gene orders of Spionidae were found to be relatively conservative (Fig. S3). In clade 1, *P. hoplura* and *Boccardiella hamata* belonged to the *Polydora*-complex with consistent gene orders, and both lacked the *atp8* gene. In clade 2, the gene orders between *R.* aff. *asiatica* and *M. neglecta* differed by a transposition in the *trnG-cox3-trnY-trnQ-trnW-nad4-cytb-atp6-trnS2-trnH-trnR* block. The gene order of *Lindaspio* sp. (NES) was found to be identical to *M. neglecta* with 13 PCGs, 22 tRNAs, and 2 rRNAs. Tandem-duplication-random-losses were observed in the mitogenome of *L. polybranchiata*. The gene arrangement of *L. polybranchiata* was identical to *Lindaspio* sp. (NES) and *M. neglecta*, with the exception of the lack of tRNA Gln.

3.2.3. Genetic diversity and past demographic changes

The genetic diversity and population dynamics of the *L. polybranchiata* population were evaluated using the mitogenomes of 8 individuals. Analysis of the 13 PCGs revealed a low level of genetic diversity, with a nucleotide diversity (Pi) of 0.00111 ± 0.00039. The value of Fu's *Fs* statistic was slightly negative but insignificant (−1.82951, p = 0.095). However, Taji-

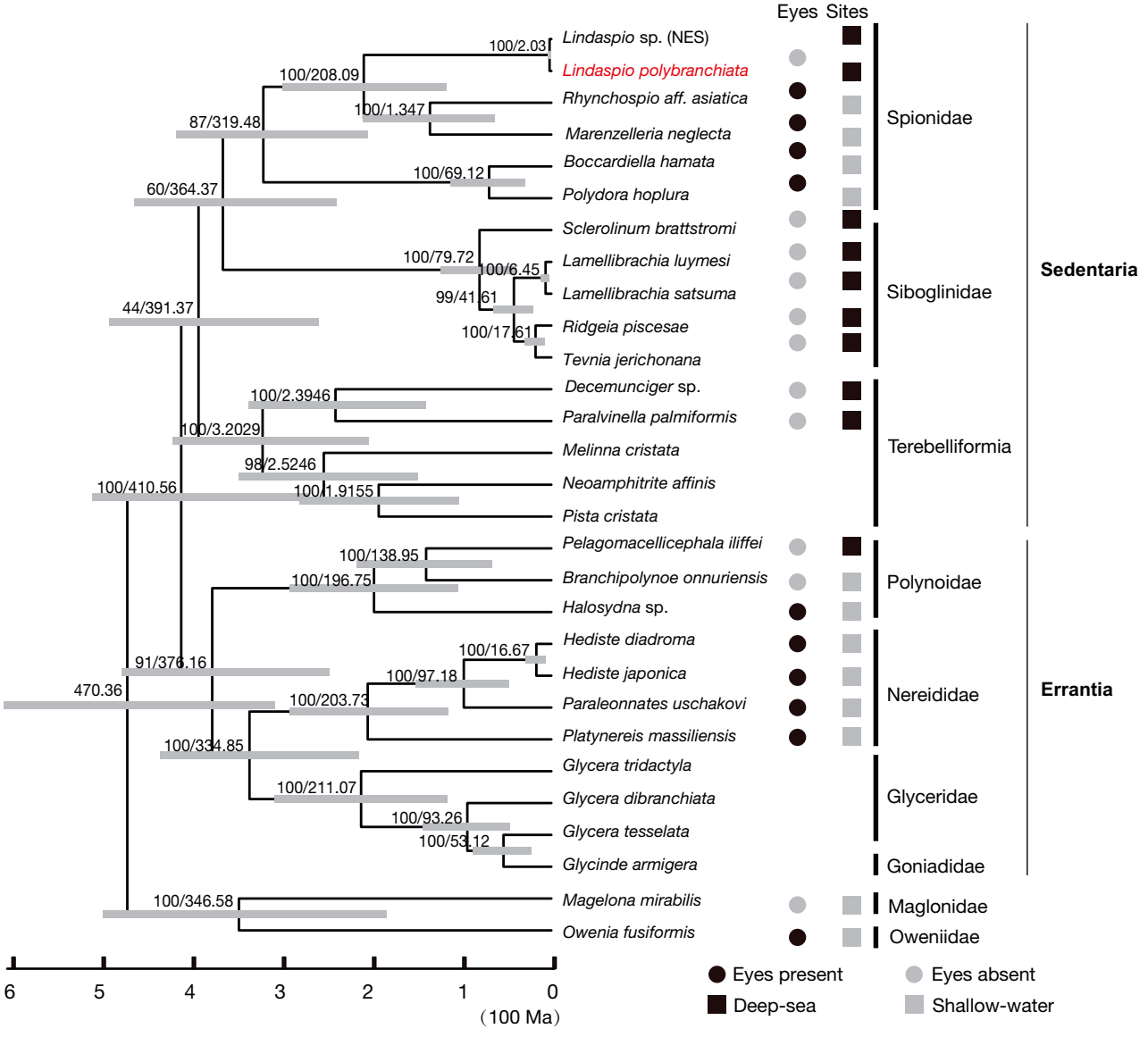

Fig. 3. Maximum likelihood phylogenetic tree inferred from the concatenated sequences of 12 mitochondrial protein-coding genes (PCGs) and 2 ribosomal RNA genes with the GTR substitution model. The first value on each node indicates the percentage bootstrap value with 1000 replications, and the second number indicates the posterior mean divergence time, with 95% highest posterior density labeled with grey lines. The grey and black circles indicate the absence and presence of eyespots, respectively. The grey and black rectangles indicate polychaetes in shallow water and in the deep sea, respectively

ma's D test and Fu & Li's D^* were significantly less than 0, rejecting the null hypothesis of neutrality theory (Table S5). The negative values indicated a possible population expansion. The mismatch distribution analysis revealed that the estimated effective population size after population growth was significantly larger than that before growth. The sum of squared deviation was 0.022 with a p-value of 0.801, suggesting no significant differences between the observed and simulated values. Harpending's raggedness index (r) was 0.033 with a p-value of 0.898, which also suggested a very good fit of the empirical data to the growth model. These findings supported a close correspondence between the population dynamics and the expected recent expansion model.

3.2.4. Positive selection analysis

The rates of synonymous (dS) and nonsynonymous (dN) substitutions were estimated using the CodeML program to determine adaptive evolution in the

Table 2. Analyses of selective pressure of the 12 mitochondrial protein-encoding genes of spionids. See Section 3.2.4 for more details

Model	lnL	Parameter estimates	Models compared	2ΔL	p
1-ratio	−72012.965120	ω0 = 0.02762	2-ratio vs. 1-ratio	6.455296	0.011
2-ratio	−72009.737472	ω1 = 0.02880 ω2 = 0.05349	Free-ratio vs. 1-ratio	187.9795	<0.0001
Free-ratio	−71918.975380				

mitogenome of the deep-sea polychaete *L. polybranchiata*. Since *atp8* is missing in the mitogenomes of *B. hamata* and *P. hoplura*, the other 12 mitochondrial PCGs were subjected to positive selection analysis using the ML tree constructed with sequences of 6 spionids and 2 terebellids (Fig. S3).

In the Phylogenetic Analysis by Maximum Likelihood (PAML) branch model, the '1-ratio', 'free-ratio', and '2-ratio' models for 12 concatenated PCGs passed the likelihood ratio test (Table 2). The '1-ratio' model means a single ω0 ratio for all branches in the phylogenetic tree; 'free ratio' means one ω ratio for each branch; and '2 ratios' means a ω2 ratio for the *Lindaspio* branch and a ω1 ratio for all other branches as background lineages. There were significant differences between the '1-ratio' and 'free-ratio' models ($p < 0.0001$), indicating that the 'free-ratio' model fits the data significantly better than the '1-ratio' model. Furthermore, the likelihood ratio tests between '1-ratio' and '2-ratio' models showed that the evolutionary rates of the deep-sea *L. polybranchiata* branch were significantly different from those of other shallow-water species, with $p = 0.011$ and ω2 (0.05349) nearly twice as large as ω1 (0.02880). These tests supported that the mitochondria of deep-sea spionids may have undergone positive selection. The positively selected sites in the mitogenome of the deep-sea *L. polybranchiata* branch were identified in the branch-site model. Twelve residues were identified as positive selection sites with Bayes empirical Bayes values >95% located in *cox1* (98 A, 292 T, 404 S, and 461 S), *cox3* (19 S and 76 S), *cytb* (349 I), and *nad5* (45 I, 168 C, 291 A, 404 S, and 541 S) in the deep-sea *L. polybranchiata* branch (Table 3).

The functional domains of these 4 positively selected PCGs were explored to identify the significance of these positively selected sites. All 12 positively selected sites were located within the functional domains of these proteins, and 4 of 12 sites were in the transmembrane domain while the remaining sites were in other domains. The 3D structures of these PCGs are presented in Fig. S4, with positive selection sites mapped onto these PCGs.

3.3. Morphological adaptations of *L. polybranchiata*

3.3.1. Morphological comparison of sensory organs

The sensory structures of *L. polybranchiata* are relatively simple. *L. polybranchiata* has no nuchal organ and eyespots, but has a well-developed caruncle, a mid-dorsal extension of the prostomium, to perceive external stimuli (Fig. 4B). We compared *L. polybranchiata* with the intertidal spionid *R.* aff. *asiatica* and found great differences in external morphology, especially the sensory organs (Table 4). In terms of photoreceptors, eyespots are absent in *L. polybranchiata* (Fig. 4A); however, *R.* aff. *asiatica* has 2 pairs of brownish eyespots arranged in a trapezoid pattern. The ante-

Table 3. Analyses of the selective pressure of the 12 mitochondrial protein-encoding genes of spionids with branch-site model. The 12 positive selection sites were identified in the deep-sea *Lindaspio*. BEB: Bayes Empirical Bayes; *: 0.95 < BEB value < 0.99; **: BEB value < 0.99. See Section 3.2.4 for more details

Gene	Positive selection sites	Amino acid	BEB value	Domain	Description
cox1	98	A	0.983*	Transmembrane	Helical
	292	T	0.968*	Other	COX1
	404	S	0.977*	Other	COX1
	461	S	0.981*	Transmembrane	Helical
cox3	19	S	0.962*	Transmembrane	Helical
	76	S	0.988*	Other	COX3
cytb	349	I	0.993**	Other	CYTB_CTER
nad5	45	I	0.953*	Transmembrane	Helical
	168	C	0.982*	Other	Proton_antipo_M
	291	A	0.955*	Other	Proton_antipo_M
	404	S	0.966*	Other	Proton_antipo_M
	541	S	0.972*	Other	NADH5_C

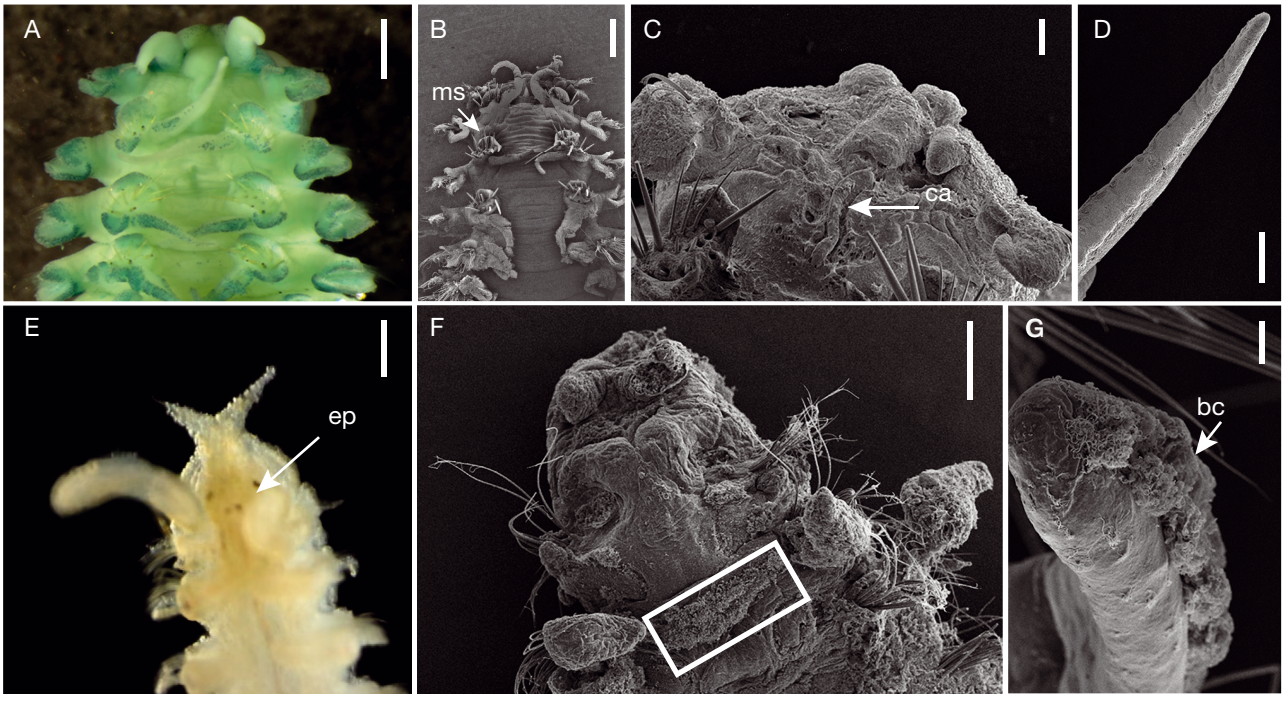

Fig. 4. Morphological features of *Lindaspio polybranchiata* and *Rhynchospio* aff. *asiatica*. (A) Modified notopodial spines of *L. polybranchiata*. (B) Anterior region of *L. polybranchiata*. (C) Detail of the prostomium in *L. polybranchiata*, dorsal view. (D) Dorsal branchia of *L. polybranchiata* in anterior chaetiger. (E,F) Anterior end of *R.* aff. *asiatica*, dorsal view; white rectangle in panel F indicates transverse ciliary row. (G) Dorsal branchia of *R.* aff. *asiatica*. ms: dorsal modified spines; ca: caruncle; ep: eyespots; bc: branchial cilia. Scale bars: A,C,E: 500 µm; B,D,F: 100 µm; G: 5 µm

Table 4. Comparison of the morphological characteristics of *Lindaspio polybranchiata* and *Rhynchospio* aff. *asiatica*

Species	Sensory organs		Respiratory structures		
	Eyespots	Caruncle	Dorsal branchiae	Ventral branchiae	Gill surface area ($cm^2\ g^{-1}$ wet weight)
Lindaspio polybranchiata	Absent	Elevated above prostomium, reaching to anterior margin of chaetiger 2	Present	Present	31.41
Rhynchospio aff. *asiatica*	2 pairs	Not elevated above prostomium, reaching to chaetiger 1	Present	Absent	24.49

rior pair is larger, the posterior is punctate and smaller, and the distance between the anterior eyespots is much greater than that between posterior eyespots (Fig. 4E). Similar to *L. southwardorum*, *L. polybranchiata* possesses a narrow caruncle with a smooth surface and extending to the anterior edge of chaetiger 2 (Fig. 4C). However, the caruncle of *R.* aff. *asiatica* is indistinct and not elevated above the prostomium (Fig. 4F).

3.3.2. Morphological comparison of respiratory structures

Lindaspio is an exclusive genus in the family Spionidae with dorsal branchiae and ventral branchiae (Fig. 5A1–A4). The surfaces of all branchiae of *L. polybranchiata* are smooth and lack cilia (Fig. 4D). Similar to most common polychaetes, *R.* aff. *asiatica* bears only dorsal branchiae that are slender and distally tapered (Fig. 5B1–B4), and the surfaces of the branchiae are densely tomentose (Fig. 4G).

The surface areas of the branchiae on the anterior, middle, and posterior segments of the body exhibit certain differences. We calculated the mean and standard deviation of surface area of single dorsal and ventral branchiata in every specimen, and further analyzed the relationship between surface area and body size. In *L. polybranchiata*, the surface areas of the single dorsal branchia vary from 0.522 ± 0.108 to 1.504 ± 0.358 mm^2, whereas those of ventral branchia

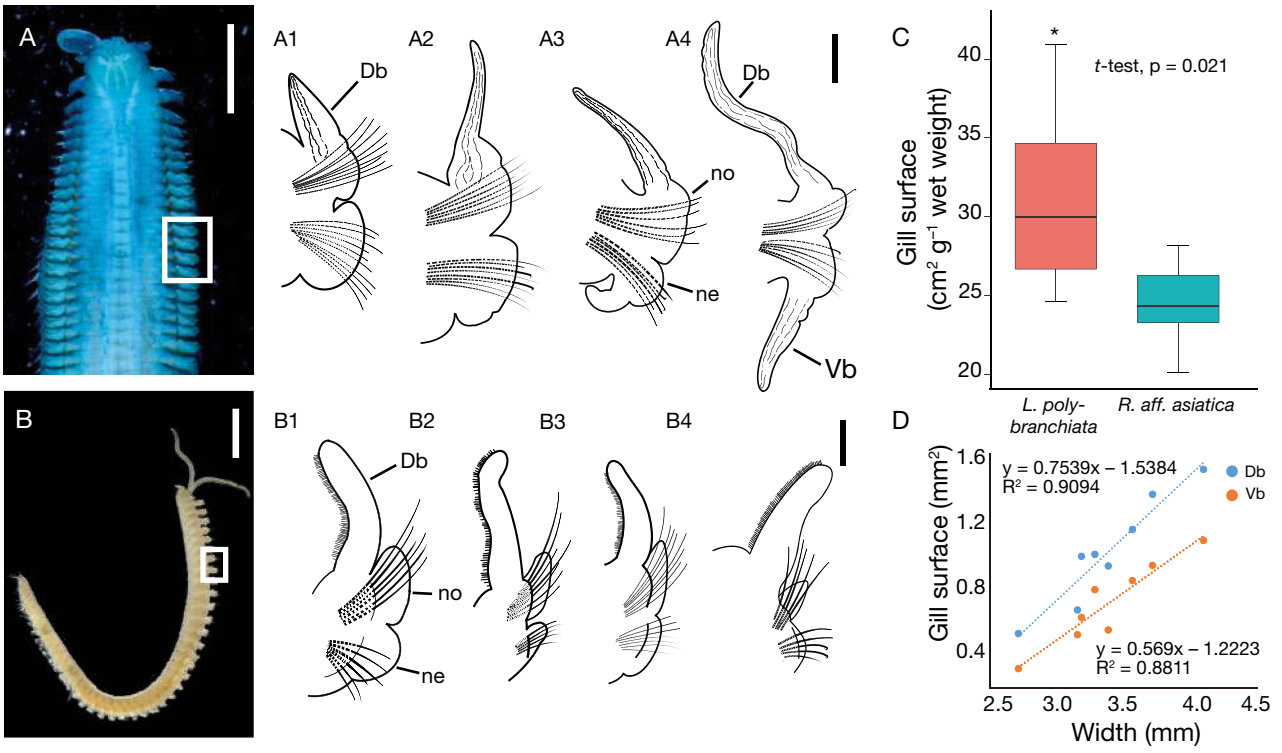

Fig. 5. Comparison of gill characteristics of *Lindaspio polybranchiata* and *Rhynchospio* aff. *asiatica*. (A) Ventral view of *L. polybranchiata*. The parapodia are indicated by the white rectangle. (B) Lateral view of *R.* aff. *asiatica*. The parapodia are indicated by the white rectangle. (A1–A4) Right back view of the parapodia in chaetiger 4, 20, 35, and 47, respectively, of *L. polybranchiata*; (B1–B4) Right back view of parapodia in chaetiger 2, 5, 25, and 45, respectively, of *R.* aff. *asiatica*. Scale bars: A,B: 1000 µm; A1–A4: 400 µm; B1–B4: 100 µm. Db: dorsal branchiae; Vb: ventral branchiae; no: notopodium; ne: neuropodium. (C) Mean gill surface in *L. polybranchiata* (from the South China Sea, SCS) and *R.* aff. *asiatica*. The asterisk indicates a significant difference ($p < 0.05$) between the 2 species. Boxplot: upper hinge: 75th percentile; lower hinge: 25th percentile; mid-line: median; whiskers: points within 1.5× interquartile range. (D) Average surface of single dorsal branchiae (Db) and ventral branchiae (Vb) in *L. polybranchiata* (SCS)

vary from 0.311 ± 0.053 to 1.070 ± 0.121 mm^2, and are positively correlated with the size of the specimens (dorsal branchia: $r = 0.954$, $p < 0.001$; ventral branchia: $r = 0.939$, $p < 0.001$; Fig. 5D). The specific branchial surface areas of *L. polybranchiata* and *R.* aff. *asiatica* were calculated by dividing the total branchial area by the wet weight. The total branchial surface areas of *L. polybranchiata* and *R.* aff. *asiatica* are 31.41 and 24.49 cm^2 per g wet weight, respectively. The branchial surface areas of these 2 species were compared using *t*-tests, and the results indicated that the respiratory surface area of *L. polybranchiata* is significantly larger than that of *R. aff. asiatica* ($p = 0.021$; Fig. 5C).

4. DISCUSSION

This study is the first to report the discovery of a dense population of *Lindaspio polybranchiata* in the western Pacific Ocean. In the present study, we assembled the mitochondrial genome of *L. polybranchiata*, established its phylogenetic position, revealed its possible evolutionary origin, analyzed population genetic diversity, and provided evidence for molecular and morphological adaptation to the deep-sea extreme environment.

Phylogenetic analysis supported that deep-sea *Lindaspio* may have originated from the invasion of shallow-sea spionids. The divergence time between the deep-sea *Lindaspio* and shallow-water spionids was estimated to be approximately 208.09 Ma, with a 95% confidence interval of 116.33–297.89 Ma (Fig. 3), which is comparable to the divergence time between deep-sea and shallow-water polynoid scale worms (ca. 120 Ma) (He et al. 2023). The divergence between the deep-sea and shallow-water spionids approximately coincided with the Triassic–Jurassic transition, which was marked by a mass extinction event that contributed to the rapid divergence of both deep-sea and shallow-water taxa (Hesselbo et al. 2002). Climate change, ocean acidification, and extensive hyp-

oxia led to the massive extinction of deep-sea faunas, creating new opportunities for the spatial divergence of shallow-water species (Greene et al. 2012). Analysis of the evolutionary origins suggested that deep-sea echinoderms, mollusks, and crustaceans were probably re-established via the invasion from adjacent shallow-water regions following extinction events (Lorion et al. 2013, Woolley et al. 2016).

The results further revealed that the *L. polybranchiata* population in the Lingshui cold seep has a low nucleotide diversity. Fu's *Fs* test statistic is based on Ewens' sampling distribution, which has low values with the excess of singleton mutations resulting from the expansion event (Ramos-Onsins & Rozas 2002). The successful colonization of the new habitat by *L. polybranchiata* might have been driven by an accumulation of new rare mutations. This could explain the slightly negative but insignificant value of Fu's *Fs* statistic for this *L. polybranchiata* population. The negative values of the neutrality test statistics and the results of mismatch analysis suggested that *L. polybranchiata* possibly underwent a recent population expansion following a bottleneck or founder event (Teixeira et al. 2011). We propose that this *L. polybranchiata* population was more likely shaped by the founder effect, and the recent population expansion was possibly associated with methane seepage.

Mitochondria are the centers of aerobic metabolism, and several studies have elucidated the unique evolutionary adaptations of the mitogenomes of organisms thriving in extreme environments such as hypoxia and energy starvation (Ruiz-Pesini et al. 2004, Meiklejohn et al. 2007, Tomasco & Lessa 2011). In the present study, several residues in the mitogenome were found to be potentially under positive selection in the foreground branch of the deep-sea *Lindaspio* (Table 3). The mutations were identified in key components of the electron transport chain, which could have potential physiological effects (Luo et al. 2008). Five positively selected residues were detected in *nad5*, and these residues mapped to functional domains. The NADH dehydrogenase complex functions as a proton pump in the respiratory chain and is an important site for the production of superoxide; therefore, mutations may affect the efficiency of the proton pump (da Fonseca et al. 2008, Yu et al. 2011). A previous study demonstrated that *nad1–5* of the family Alvinocarididae dwelling in hydrothermal vents were under positive selection in response to the highly toxic chemicals and hypoxic environment (Sun et al. 2018). One residue was identified as positively selected in the *cytb* gene. Cytochrome *b*, a key component of *bc*1, participates in oxidative phosphorylation in the mitochondrial membrane and catalyzes reversible electron transfer from ubiquinol to cytochrome *c* coupled to proton translocation (Trumpower 1990). Cytochrome *c* oxidase is the terminal oxidase of the mitochondrial electron transport chain and catalyzes electron transfer from cytochrome *c* to molecular oxygen (Michel et al. 1998). Cytochrome *c* oxidases also reduce NO_2 to NO, which induces the expression of nuclear hypoxic genes (Castello et al. 2006). Therefore, cytochrome *c* oxidase is an important target of positive selection in the adaptation to hypoxia. Several positive selection sites have been found in the cytochrome *c* oxidase genes of numerous deep-sea organisms (Shen et al. 2019, Li et al. 2021, Zhang et al. 2021). In the deep-sea *L. polybranchiata* branch, 6 positive selection residues were detected in the functional domains of *cox1* and *cox3*, consistent with existing research (Dhar & Dey 2021, Yang et al. 2021). We speculate that the selection sites in the components of the electron transport chain could be involved in the adaptive evolution of deep-sea spionids.

In addition to mitogenome evolution, some key characteristics could have undergone evolution to adapt to the extremely harsh conditions in the deep sea. According to ultrastructural results, the branchiae of polychaetes function as respiratory organs that play an important role in gas exchange (Storch & Alberti 1978). To ensure normal physiological activities in a hypoxic environment, many polychaetes may increase the surface area of the gills and develop dorsal branchiae of various shapes for the efficient uptake of oxygen (Lucey et al. 2020). The genus *Lindaspio* has elaborate development of both dorsal and ventral branchiae (Fig. 5A4), which is unique among spionids and polychaetes (Sigvaldadóttir et al. 1997). The respiratory surface area of *L. polybranchiata* in 1800 m was 31.41 $cm^2\ g^{-1}$ wet weight, which was significantly larger than that of its close relative *R.* aff. *asiatica* in shallow water. It has been reported that the surface area of gills increases in several polychaetes dwelling in hydrothermal vents and cold seeps. In Polynoidae, littoral species usually lack gills; however, the majority of species in hydrothermal vents and cold seeps have well-developed gills (Hourdez & Jouin-Toulmond 1998). The gill surface area of *Paralvinella grasslei* in white and black smokers at 2600 m depth is 47 $cm^2\ g^{-1}$ wet weight, the largest known in polychaetes (Jouin & Gaill 1990). This increase in the respiratory surface area has also been reported in benthic invertebrates for facilitating gas exchange in oxygen minimum zones around the world (Lamont & Gage 2000).

Owing to the permanent darkness, the reduction of eyes is a common phenomenon in the deep sea and is especially common among polychaetes. Nearly all polychaetes dwelling in caves (genus *Branchipolynoe*) and deep-sea environments (genera *Branchinotogluma*, *Lepidonotopodium*, and *Levensteiniella*) have lost their eyes (Gonzalez et al. 2021). Based on our phylogenetic analysis, the presence of eyespots was an ancestral character in the last common ancestor of the examined taxa (Fig. 3). The loss of eyespots may be a result of independent evolution in the deep sea due to permanent darkness (Sigvaldadóttir & Desbruyeres 2003, Hourdez et al. 2006, Blake & Ramey-Balci 2020). Meanwhile, deep-sea taxa have enhanced sensory organs that resulted from convergent evolution (Gonzalez et al. 2021). These key adaptive traits are exemplified in *L. polybranchiata*, which has lost its eyespots but possesses a highly developed caruncle. The caruncle is a bulging dorsal sensory area arising from the prostomium, and is filled with epidermal and nervous tissue (Schlötzer-Schrehardt 1987, Buhre & Purschke 2021). The caruncle is an important chemoreceptor (Schlötzer-Schrehardt 1986) that may contribute to the high population density of *L. polybranchiata* in methane seepages.

These adaptive features enable *L. polybranchiata* to detect chemical clues within chemosynthetic ecosystems, tolerate extreme conditions, and rapidly colonize this new cold seep. Considering the overwhelming abundance compared with other metazoans in the local ecosystem, we propose that *L. polybranchiata* might be a potential pioneer species in this nascent active cold seep. Pioneer species are distinguished by high dispersal ability, rapid recruitment, short life cycles, fast growth rate, low reproductive age, and high fecundity, and these characteristics apply to varying degrees to the members of the family Spionidae (Poorter et al. 2023). The Lingshui cold seep is in its infant stage, and all species, including *L. polybranchiata*, are concentrated in small spots around the seepage. All *Lindaspio* discovered so far are distributed in chemosynthetic ecosystems. *L. polybranchiata* was therefore considered as a pioneer species in the Lingshui cold seep. Megafauna have received more attention in previous studies than sediment-dwelling infauna, and vestimentiferan tubeworms and mollusk gastropods were inferred to be candidate pioneer species in deep-sea chemosynthetic ecosystems (Fisher et al. 1997, Mullineaux et al. 2010, Van Dover 2014). The Congo deep-sea fan is located on the Congo–Angola margin in the South Atlantic Ocean, and it hosts multiple chemosynthesis-based communities (Pruski et al. 2017). By analyzing the spatial variability of the cold-seep-like macrofaunal communities in the Congo deep-sea fan, Olu et al. (2017) proposed a possible succession model for cold-seep communities, in which the first colony consists of opportunistic, motile, and sulfide-tolerant polychaetes, namely, dorvilleids and hesionids. Our report of the infauna polychaete *L. polybranchiata* as a candidate pioneer species is consistent with the community succession model in the Congo deep-sea fan.

L. polybranchiata worms burrow deep into bottom sediments and form large numbers of loose tubes. A previous study indicated that the burrowing behavior of *Marenzelleria* worms caused bioturbation and bioirrigation of the bottom sediments (Golubkov et al. 2021). It can be suggested that these burrows introduce oxygen-rich and sulfate-rich waters deep into the sediments, promoting high microbial metabolic rates in sediments and accelerating the process of community succession (Gibson et al. 2005). Additionally, bioirrigation can modify the physical, chemical, and biological characteristics of the bottom sediments, and create a positive environment for colonization by other organisms (Braeckman et al. 2010, Daunys et al. 2019). In the Congo lobe complex, located on the Congo–Angola margin, the first colonizers, dorvilleids and hesionids, burrowed to 5–10 cm depth. Bioirrigation enhances the consumption of sulfides by sulfur-oxidizing bacteria, decreases the sulfide concentration in the upper sediment layers, and creates favorable conditions for the settlement of vesicomyid juveniles (Olu et al. 2017). The large biomass of *L. polybranchiata* guarantees an adequate supply of food to subsequent organisms. Therefore, *L. polybranchiata* is an ecologically important taxon that may lay the foundation layer for the establishment and succession of cold seep communities in the early stage. Therefore, further studies are necessary to enhance our understanding of the ecological function of such pioneer species and the interaction between *L. polybranchiata* and other organisms.

5. CONCLUSIONS

In this study, we have reported a dense population of *Lindaspio polybranchiata* in a newly established cold seep with vigorous methane bubbling. We outlined the mitochondrial genome, established the phylogenetic position, and analyzed the population genetic diversity. Our findings provide a genomic baseline for subsequent studies. The mitogenome of *L. polybranchiata* is 15 248 bp long and contains 13 PCGs, 21

tRNAs, 2 rRNAs, and 1 CR. Phylogenetic analysis revealed that the ancestor of the deep-sea *Lindaspio* originated from shallow-water spionids, and the divergence time corresponded to the Triassic–Jurassic mass extinction. The potential adaptive responses of *Lindaspio* to the harsh deep-sea conditions were also determined by comparative analyses of the mitogenome and morphology of offshore and deep-sea spionids. In the deep-sea *Lindaspio* branch, 12 residues in *cox1*, *cox3*, *cytb*, and *nad5* were found to be potentially under positive selection. It could be speculated that these positively selected sites may play an important role in the adaptation of *L. polybranchiata*. Compared with the inshore species, the ventral branchiae and specific respiratory surface areas of *L. polybranchiata* are significantly enlarged in response to hypoxia for facilitating oxygen acquisition. Additionally, the eyespots of *L. polybranchiata* have undergone degeneration, whereas the caruncle is well developed, which may aid in perceiving chemical clues in the surrounding environment. This study is the first to investigate the adaptation of the deep-sea genus *Lindaspio* that is endemic to chemosynthetic ecosystems, and provides morphological and molecular insights for further comparative studies.

Data availability. The mitogenome sequence data that support the findings of this study are openly available in NCBI GenBank at https://www.ncbi.nlm.nih.gov/ under accession nos. OK032597, BK062759, and OP288981. The alignment sequences for phylogenetic analysis are available in Figshare (https://doi.org/10.6084/m9.figshare.24588333.v1).

Acknowledgements. We appreciate the assistance provided by the crews of RV 'Kexue'. We are also grateful to Lei Cao and Chao Lian for their help in providing environmental data. This work was supported by the National Natural Science Foundation of China (42030407 and 42076091), the NSFC Innovative Group Grant (42221005), Marine S&T Fund of Shandong Province for Pilot National Laboratory for Marine Science and Technology (Qingdao) (2022QNLM030004), and the Strategic Priority Research Program of the Chinese Academy of Sciences (XDB42000000).

LITERATURE CITED

Alalykina IL (2022) Composition and distribution of polychaete assemblages associated with hydrothermal vents and cold seeps in the Bering Sea. Deep Sea Res II 206: 105192

Bellan G, Dauvin JC, Laubier L (2003) The genus *Lindaspio* (Annelida: Polychaeta: Spionidae), and a new species from an oil field off Congo, western Africa. J Nat Hist 37: 2413–2424

Bennett AD, Rakocinski CF (2020) Respiration by the opportunistic spionid polychaete *Streblospio gynobranchiata* during adjustment to and recovery from moderate hypoxia. Diversity 12:73

Bernt M, Donath A, Jühling F, Externbrink F and others (2013) MITOS: improved de novo metazoan mitochondrial genome annotation. Mol Phylogenet Evol 69: 313–319

Birch GF, O'Donnell MA, McCready S (2018) Complex relationships between shallow muddy benthic assemblages, sediment chemistry and toxicity in estuaries in southern New South Wales, Australia. Mar Pollut Bull 129: 573–591

Blake JA (1985) Polychaeta from the vicinity of deep-sea geothermal vents in the eastern Pacific. I: Euphrosinidae, Phyllodocidae, Hesionidae, Nereididae, Glyceridae, Dorvilleidae, Orbiniidae and Maldanidae. Bull Biol Soc Wash 6:67–101

Blake JA (2000) A new genus and species of polychaete worm (Family Orbiniidae) from methane seeps in the Gulf of Mexico, with a review of the systematics and phylogenetic interrelationships of the genera of Orbiniidae. Cah Biol Mar 41:435–441

Blake JA, Maciolek NJ (1992) Polychaeta from deep-sea hydrothermal vents in the Eastern Pacific. III: a new genus and two new species of Spionidae from the Guaymas Basin and Juan de Fuca ridge with comments on a related species from the western North Atlantic. Proc Biol Soc Wash 105:723–732

Blake JA, Ramey-Balci PA (2020) A new genus and species of spionid polychaete (Annelida, Spionidae) from a deep-water cold seep site in the Eastern Mediterranean Sea off Turkey. Zoosymposia 19:121–134

Boetius A, Wenzhöfer F (2013) Seafloor oxygen consumption fuelled by methane from cold seeps. Nat Geosci 6: 725–734

Bogantes V (2020) Diversity and evolution of annelids with emphasis on Spionidae. PhD dissertation, Auburn University, Auburn, AL

Braeckman U, Provoost P, Gribsholt B, Van Gansbeke D and others (2010) Role of macrofauna functional traits and density in biogeochemical fluxes and bioturbation. Mar Ecol Prog Ser 399:173–186

Buhre JS, Purschke G (2021) Ultrastructure and functional morphology of the dorsal organs in *Scoloplos armiger* (Annelida, Sedentaria, Orbiniida). Zoomorphology 140: 437–452

Castello PR, David PS, McClure T, Crook Z, Poyton RO (2006) Mitochondrial cytochrome oxidase produces nitric oxide under hypoxic conditions: implications for oxygen sensing and hypoxic signaling in eukaryotes. Cell Metab 3:277–287

Chen H, Parry LA, Vinther J, Zhai D, Hou X, Ma X (2020) A Cambrian crown annelid reconciles phylogenomics and the fossil record. Nature 583:249–252

Conlan KE, Kvitek RG (2005) Recolonization of soft-sediment ice scours on an exposed Arctic coast. Mar Ecol Prog Ser 286:21–42

Cordes EE, Bergquist DC, Fisher CR (2009) Macro-ecology of Gulf of Mexico cold seeps. Annu Rev Mar Sci 1:143–168

da Fonseca RR, Johnson WE, O'Brien SJ, Ramos MJ, Antunes A (2008) The adaptive evolution of the mammalian mitochondrial genome. BMC Genomics 9:119

Daunys D, Forster S, Schiedek D, Olenin S, Zettler ML (2019) Effect of species invasion on transport of solutes at different levels of soft sediment macrofauna diversity: results from an experimental approach. Water 11:1544

David AA, Williams JD (2012) Asexual reproduction and anterior regeneration under high and low temperatures in the sponge associate *Polydora colonia* (Polychaeta: Spionidae). Invertebr Reprod Dev 56:315–324

Desbruyeres D, Toulmond A (1998) A new species of hesionid worm, *Hesiocaeca methanicola* sp. nov. (Polychaeta: Hesionidae), living in ice-like methane hydrates in the deep Gulf of Mexico. Cah Biol Mar 39:93–98

Dhar D, Dey D (2021) Comparison of evolutionary selection acting on the mitochondrial protein-coding genes between intertidal and deep-sea gastropods. Int J Res Appl Sci Biotechnol 8:59–64

Excoffier L, Laval G, Schneider S (2006) Arlequin v3. 1. An integrated software for population genetic data analysis. Evolutionary Bioinformatics Online. https://www.cmpg.unibe.ch/software/arlequin3/

Fisher CR, Urcuyo IA, Simpkins MA, Nix E (1997) Life in the slow lane: growth and longevity of cold-seep vestimentiferans. Mar Ecol 18:83–94

Fontanillas E, Galzitskaya OV, Lecompte O, Lobanov MY and others (2017) Proteome evolution of deep-sea hydrothermal vent alvinellid polychaetes supports the ancestry of thermophily and subsequent adaptation to cold in some lineages. Genome Biol Evol 9:279–296

Gibson R, Atkinson R, Gordon J (2005) Ecology of cold seep sediments: interactions of fauna with flow, chemistry and microbes. Oceanogr Mar Biol Annu Rev 43:1–46

Golubkov S, Tiunov A, Golubkov M (2021) Food-web modification in the eastern Gulf of Finland after invasion of *Marenzelleria arctia* (Spionidae, Polychaeta). NeoBiota 66:75–94

Gonzalez BC, Martínez A, Worsaae K, Osborn KJ (2021) Morphological convergence and adaptation in cave and pelagic scale worms (Polynoidae, Annelida). Sci Rep 11:10718

Graff JR, Blake JA, Wishner KF (2008) A new species of *Malacoceros* (Polychaeta: Spionidae) from Kick'em Jenny, a hydrothermally active submarine volcano in the Lesser Antilles Arc. J Mar Biol Assoc UK 88:925–930

Greene SE, Martindale RC, Ritterbush KA, Bottjer DJ, Corsetti FA, Berelson WM (2012) Recognising ocean acidification in deep time: an evaluation of the evidence for acidification across the Triassic-Jurassic boundary. Earth Sci Rev 113:72–93

Guggolz T, Meißner K, Schwentner M, Brandt A (2019) Diversity and distribution of *Laonice* species (Annelida: Spionidae) in the tropical North Atlantic and Puerto Rico Trench. Sci Rep 9:9260

Guggolz T, Meißner K, Schwentner M, Dahlgren TG, Wiklund H, Bonifácio P, Brandt A (2020) High diversity and pan-oceanic distribution of deep-sea polychaetes: *Prionospio* and *Aurospio* (Annelida: Spionidae) in the Atlantic and Pacific Ocean. Org Divers Evol 20:171–187

Han Y, Zhang D, Wang C, Zhou Y (2021) Out of the Pacific: a new alvinellid worm (Annelida: Terebellida) from the northern Indian Ocean hydrothermal vents. Front Mar Sci 8:669918

He X, Wang H, Xu T, Zhang Y and others (2023) Genomic analysis of a scale worm provides insights into its adaptation to deep-sea hydrothermal vents. Genome Biol Evol 15:evad125

Hesselbo SP, Robinson SA, Surlyk F, Piasecki S (2002) Terrestrial and marine extinction at the Triassic-Jurassic boundary synchronized with major carbon-cycle perturbation: a link to initiation of massive volcanism? Geology 30:251–254

Hilário A (2005) Reproductive ecology of Vestimentifera (Polychaeta: Siboglinidae) from hydrothermal vents and cold seeps. PhD thesis, University of Southampton

Hourdez S, Jollivet D (2020) Metazoan adaptation to deep-sea hydrothermal vents. In: di Prisco G, Edwards HGM, Elster J, Huiskes AHL (eds) Life in extreme environments: insights in biological capability. Cambridge University Press, Cambridge, p 42–67

Hourdez S, Jouin-Toulmond C (1998) Functional anatomy of the respiratory system of *Branchipolynoe* species (Polychaeta, Polynoidae), commensal with *Bathymodiolus* species (Bivalvia, Mytilidae) from deep-sea hydrothermal vents. Zoomorphology 118:225–233

Hourdez S, Lallier FH (2007) Adaptations to hypoxia in hydrothermal-vent and cold-seep invertebrates. Rev Environ Sci Biotechnol 6:143–159

Hourdez S, Frederick LA, Schernecke A, Fisher CR (2001) Functional respiratory anatomy of a deep-sea orbiniid polychaete from the Brine Pool NR-1 in the Gulf of Mexico. Invertebr Biol 120:29–40

Hourdez S, Weber RE, Green BN, Kenney JM, Fisher CR (2002) Respiratory adaptations in a deep-sea orbiniid polychaete from Gulf of Mexico brine pool NR-1: metabolic rates and hemoglobin structure/function relationships. J Exp Biol 205:1669–1681

Hourdez S, Desbruyères D, Laubier L, Gardiner SL (2006) *Malacoceros samurai*, a new species of Spionidae (Annelida: Polychaeta) from hydrothermal vent chimney walls on the south East Pacific Rise. Proc Biol Soc Wash 119: 592–599

Hunt HL, Metaxas A, Jennings RM, Halanych KM, Mullineaux LS (2004) Testing biological control of colonization by vestimentiferan tubeworms at deep-sea hydrothermal vents (East Pacific Rise, 9° 50' N). Deep Sea Res I 51: 225–234

Jouin C, Gaill F (1990) Gills of hydrothermal vent annelids: structure, ultrastructure and functional implications in two alvinellid species. Prog Oceanogr 24:59–69

Kauppi L, Norkko A, Norkko J (2015) Large-scale species invasion into a low-diversity system: spatial and temporal distribution of the invasive polychaetes *Marenzelleria* spp. in the Baltic Sea. Biol Invasions 17: 2055–2074

Lamont PA, Gage JD (2000) Morphological responses of macrobenthic polychaetes to low oxygen on the Oman continental slope, NW Arabian Sea. Deep Sea Res II 47: 9–24

Li Q, Li Y, Na J, Han X and others (2021) Description of a new species of *Histampica* (Ophiuroidea: Ophiothamnidae) from cold seeps in the South China Sea and analysis of its mitochondrial genome. Deep Sea Res I 178:103658

Lo Giudice A, Rizzo C (2022) Bacteria associated with benthic invertebrates from extreme marine environments: promising but underexplored sources of biotechnologically relevant molecules. Mar Drugs 20:617

Lorion J, Kiel S, Faure B, Kawato M and others (2013) Adaptive radiation of chemosymbiotic deep-sea mussels. Proc R Soc B 280:20131243

Lucey NM, Collins M, Collin R (2020) Oxygen-mediated plasticity confers hypoxia tolerance in a corallivorous polychaete. Ecol Evol 10:1145–1157

Luo Y, Gao W, Gao Y, Tang S and others (2008) Mitochondrial genome analysis of *Ochotona curzoniae* and implication of cytochrome *c* oxidase in hypoxic adaptation. Mitochondrion 8:352–357

Meiklejohn CD, Montooth KL, Rand DM (2007) Positive and negative selection on the mitochondrial genome. Trends Genet 23:259–263

Meng G, Li Y, Yang C, Liu S (2019) MitoZ: a toolkit for animal mitochondrial genome assembly, annotation and visualization. Nucleic Acids Res 47:e63

Michel H, Behr J, Harrenga A, Kannt A (1998) Cytochrome *c* oxidase: structure and spectroscopy. Annu Rev Biophys Biomol Struct 27:329–356

Miya M, Nishida M (1999) Organization of the mitochondrial genome of a deep-sea fish, *Gonostoma gracile* (Teleostei: Stomiiformes): first example of transfer RNA gene rearrangements in bony fishes. Mar Biotechnol 1: 416–426

Mullineaux LS, Adams DK, Mills SW, Beaulieu SE (2010) Larvae from afar colonize deep-sea hydrothermal vents after a catastrophic eruption. Proc Natl Acad Sci USA 107:7829–7834

Nakajima Y, Shinzato C, Khalturina M, Nakamura M, Watanabe H, Satoh N, Mitarai S (2016) The mitochondrial genome sequence of a deep-sea, hydrothermal vent limpet, *Lepetodrilus nux*, presents a novel vetigastropod gene arrangement. Mar Genomics 28:121–126

Olu K, Decker C, Pastor L, Caprais JC and others (2017) Cold-seep-like macrofaunal communities in organic- and sulfide-rich sediments of the Congo deep-sea fan. Deep Sea Res II 142:180–196

Peterson KJ (2005) Macroevolutionary interplay between planktic larvae and benthic predators. Geology 33: 929–932

Poorter L, Amissah L, Bongers F, Hordijk I and others (2023) Successional theories. Biol Rev Camb Philos Soc 98: 2049–2077

Pruski AM, Decker C, Stetten E, Vétion G and others (2017) Energy transfer in the Congo deep-sea fan: from terrestrially-derived organic matter to chemosynthetic food webs. Deep Sea Res II 142:197–218

Quiroga E, Quiñones RA, González RR, Gallardo VA, Jessen G (2007) Aerobic and anaerobic metabolism of *Paraprionospio pinnata* (Polychaeta: Spionidae) in central Chile. J Mar Biol Assoc UK 87:459–463

Radashevsky VI (2012) Spionidae (Annelida) from shallow waters around the British Islands: an identification guide for the NMBAQC Scheme with an overview of spionid morphology and biology. Zootaxa 3152:1–35

Ramos-Onsins SE, Rozas J (2002) Statistical properties of new neutrality tests against population growth. Mol Biol Evol 19:2092–2100

Reuscher M, Fiege D, Wehe T (2012) Terebellomorph polychaetes from hydrothermal vents and cold seeps with the description of two new species of Terebellidae (Annelida: Polychaeta) representing the first records of the family from deep-sea vents. J Mar Biol Assoc UK 92: 997–1012

Rinke C, Lee RW (2009) Pathways, activities and thermal stability of anaerobic and aerobic enzymes in thermophilic vent paralvinellid worms. Mar Ecol Prog Ser 382: 99–112

Rozas J, Ferrer-Mata A, Sanchez-DelBarrio JC, Guirao-Rico S, Librado P, Ramos-Onsins SE, Sanchez-Gracia A (2017) DnaSP 6: DNA sequence polymorphism analysis of large data sets. Mol Biol Evol 34:3299–3302

Ruiz-Pesini E, Mishmar D, Brandon M, Procaccio V, Wallace DC (2004) Effects of purifying and adaptive selection on regional variation in human mtDNA. Science 303:223–226

Schlötzer-Schrehardt U (1986) Ultrastructural investigation of the nuchal organs of *Pygospio elegans* (Polychaeta). I. Larval nuchal organs. Helgol Meeresunters 40:397–417

Schlötzer-Schrehardt U (1987) Ultrastructural investigation of the nuchal organs of *Pygospio elegans* (Polychaeta) II. Adult nuchal and dorsal organs. Zoomorphology 107: 169–179

Sellanes J, Quiroga E, Gallardo VA (2004) First direct evidence of methane seepage and associated chemosynthetic communities in the bathyal zone off Chile. J Mar Biol Assoc UK 84:1065–1066

Shank TM, Fornari DJ, Von Damm KL, Lilley MD, Haymon RM, Lutz RA (1998) Temporal and spatial patterns of biological community development at nascent deep-sea hydrothermal vents (9 50′ N, East Pacific Rise). Deep Sea Res II 45:465–515

Shen X, Pu Z, Chen X, Murphy RW, Shen Y (2019) Convergent evolution of mitochondrial genes in deep-sea fishes. Front Genet 10:925

Sigvaldadóttir E, Desbruyeres D (2003) Two new species of spionidae (Annelida: Polychaeta) from Mid-Atlantic ridge hydrothermal vents. Cah Biol Mar 44:219–225

Sigvaldadóttir E, Mackie AS, Pleijel F (1997) Generic interrelationships within the Spionidae (Annelida: Polychaeta). Zool J Linn Soc 119:473–500

Stamatakis A (2014) RAxML version 8: a tool for phylogenetic analysis and post-analysis of large phylogenies. Bioinformatics 30:1312–1313

Storch V, Alberti G (1978) Ultrastructural observations on the gills of polychaetes. Helgol Wiss Meeresunters 31: 169–179

Sui J, Dong D, Wu X, Li X (2023) A new species of the genus *Lindaspio* Blake & Maciolek, 1992 (Annelida, Spionidae) from a cold seep near Hainan Island, China. ZooKeys 1153:105–112

Sumida PYG, Alfaro-Lucas JM, Shimabukuro M, Kitazato H and others (2016) Deep-sea whale fall fauna from the Atlantic resembles that of the Pacific Ocean. Sci Rep 6: 22139

Sun S, Hui M, Wang M, Sha Z (2018) The complete mitochondrial genome of the alvinocaridid shrimp *Shinkaicaris leurokolos* (Decapoda, Caridea): insight into the mitochondrial genetic basis of deep-sea hydrothermal vent adaptation in the shrimp. Comp Biochem Physiol D Genomics Proteomics 25:42–52

Sun Y, Sun J, Yang Y, Lan Y and others (2021) Genomic signatures supporting the symbiosis and formation of chitinous tube in the deep-sea tubeworm *Paraescarpia echinospica*. Mol Biol Evol 38:4116–4134

Tamura K, Stecher G, Kumar S (2021) MEGA11: molecular evolutionary genetics analysis version 11. Mol Biol Evol 38:3022–3027

Teixeira S, Cambon-Bonavita MA, Serrão EA, Desbruyéres D, Arnaud-Haond S (2011) Recent population expansion and connectivity in the hydrothermal shrimp *Rimicaris exoculata* along the Mid-Atlantic Ridge. J Biogeogr 38: 564–574

Tomasco IH, Lessa EP (2011) The evolution of mitochondrial genomes in subterranean caviomorph rodents: adaptation against a background of purifying selection. Mol Phylogenet Evol 61:64–70

Trumpower BL (1990) The protonmotive Q cycle: energy transduction by coupling of proton translocation to electron transfer by the cytochrome bc_1 complex. J Biol Chem 265:11409–11412

Van Dover CL (2014) Impacts of anthropogenic disturbances at deep-sea hydrothermal vent ecosystems: a review. Mar Environ Res 102:59–72

Woolley SNC, Tittensor DP, Dunstan PK, Guillera-Arroita G and others (2016) Deep-sea diversity patterns are shaped by energy availability. Nature 533:393–396

Yachdav G, Kloppmann E, Kajan L, Hecht M and others (2014) PredictProtein — an open resource for online prediction of protein structural and functional features. Nucleic Acids Res 42:W337–W343

Yang M, Dong D, Li X (2021) The complete mitogenome of *Phymorhynchus* sp. (Neogastropoda, Conoidea, Raphitomidae) provides insights into the deep-sea adaptive evolution of Conoidea. Ecol Evol 11:7518–7531

Yang Z (2007) PAML 4: phylogenetic analysis by maximum likelihood. Mol Biol Evol 24:1586–1591

Yang Z, Rannala B (2006) Bayesian estimation of species divergence times under a molecular clock using multiple fossil calibrations with soft bounds. Mol Biol Evol 23: 212–226

Yu L, Wang X, Ting N, Zhang Y (2011) Mitogenomic analysis of Chinese snub-nosed monkeys: evidence of positive selection in NADH dehydrogenase genes in high-altitude adaptation. Mitochondrion 11:497–503

Zhang K, Sun J, Xu T, Qiu JW, Qian PY (2021) Phylogenetic relationships and adaptation in deep-sea mussels: insights from mitochondrial genomes. Int J Mol Sci 22: 1900

Editorial responsibility: Inna Sokolova, Rostock, Germany
Reviewed by: 3 anonymous referees

Submitted: August 30, 2023
Accepted: January 2, 2024
Proofs received from author(s): March 2, 2024